ELSEVIER

Physica B 283 (2000) 343–354

PHYSICA B

www.elsevier.com/locate/physb

Added flexibility in triple axis spectrometers: the two RITAs at Risø

K. Lefmann[a,*], D.F. McMorrow[a], H.M. Rønnow[a], K. Nielsen[a], K.N. Clausen[a], B. Lake[b], G. Aeppli[a,c]

[a]*Condensed Matter Physics and Chemistry Department, Risø National Laboratory, Frederiksborgvej 399, DK-4000 Roskilde, Denmark*
[b]*Oak Ridge National Laboratory, Oak Ridge, TE 37831, USA*
[c]*NEC Research, 4 Independence Way, Princeton, NJ 08540, USA*

Abstract

The cold-neutron triple-axis spectrometer RITA-1 at Risø has been operational for about three years, and in the near future an improved version, RITA-2, will replace the existing triple-axis instrument TAS7. We review the performance of RITA-1 and the operation modes of its flexible secondary spectrometer, giving examples of a few key experiments, and describe the software developed for running it. Further, the design of the new RITA-2 instrument is presented. The two RITA spectrometers are compared with their sister instrument SPINS at NIST and with similar instruments planned elsewhere.

Keywords: Neutron instrumentation

1. Introduction

The conventional triple-axis spectrometer (TAS) has been the main work-horse for investigations of excitations in condensed matter. Advantages of the TAS include the relatively simple design and the ability to make efficient use of the incident flux to examine particular points in $(\boldsymbol{q}, \hbar\omega)$ space. Correspondingly, its chief weakness is that only a small fraction of the scattered beam is detected, with the result that the TAS is inefficient for surveying large volumes of $(\boldsymbol{q}, \hbar\omega)$ space. Steady progress in the performance of the TAS was achieved over the years through the introduction of focusing optics, etc., but attempts to radically change the design were unsuccessful, due to background problems and/or an overwhelming complexity (see Ref. [1] and references therein). Improvements in detector technology and neutron-optical components, allied with the continued increase in computer power, has led to recent initiatives at several institutes to rethink the basic TAS design. The first instruments based on this approach are RITA-1 at Risø [1–3] and SPINS at NIST [4,5], while others are under construction or in the planning phase.

The advantages of this new generation of TAS include a higher incident flux owing to improvements in neutron guides, a higher background suppression from better shielding materials,

* Corresponding author. Tel.: +45-46-77-47-26; fax: +45-4677-4790.
E-mail address: kim.lefmann@risoe.dk (K. Lefmann).

0921-4526/00/$ - see front matter
PII: S0921-4526(00)00335-5

and, most importantly, a flexible secondary spectrometer which uses a multi-blade analyser system in combination with a position-sensitive detector (PSD). This last feature opens up the possibility of configuring the spectrometer optimally for each new type of experiment. Overall, the gain factor that can be achieved with these new spectrometers can be estimated from the factor 2–4 for the increase in incident flux, multiplied by a further factor (~ 5) for the increase in solid angle covered by the secondary spectrometer. Of course, the increased flexibility comes at a price of an increase in the complexity of both the control software and subsequent data analysis. However, it has already been demonstrated that these problems can be overcome, and experiments are being performed that would either be impossible with conventional TAS or would require unreasonable amounts of beam time.

This paper deals mainly with the two Risø spectrometers, RITA-1 and RITA-2. The former was commisioned in early 1997, and most of the features of its primary spectrometer are now understood. We will concentrate on the configurations of the secondary spectrometer, which is still in an exploratory phase, and show a few examples of recent experiments in different configurations. RITA-2 is expected to be commisioned in the summer of 2000. We describe the design of the spectrometer and compare it with RITA-1. We begin the paper with a general section on configurations of a multi-blade analyser system, and at the end of the paper, we briefly present developments of flexible TAS on other neutron sources.

2. Modes of running a flexible analyser system

A RITA-type analyser system consists of a linear assembly and a number of equidistant analyser blades mounted on the assembly. We name the rotation angle of the assembly by Ψ, the relative rotation of blade i is denoted by χ_i, $2\theta_A$ is the scattering angle, l_{SA} is the sample-analyser distance, and l_{AD} is the analyser–detector distance. The geometry and the rotation angles are illustrated in Fig. 1. The distance from the assembly centre to the centre of blade i is denoted d_i and is positive in the direction shown in the figure. For this type of analyser system, we have identified a number of operation modes, focused or dispersive, which are either currently in use on RITA-1 or SPINS, or have been proposed elsewhere [1,3,6,7].

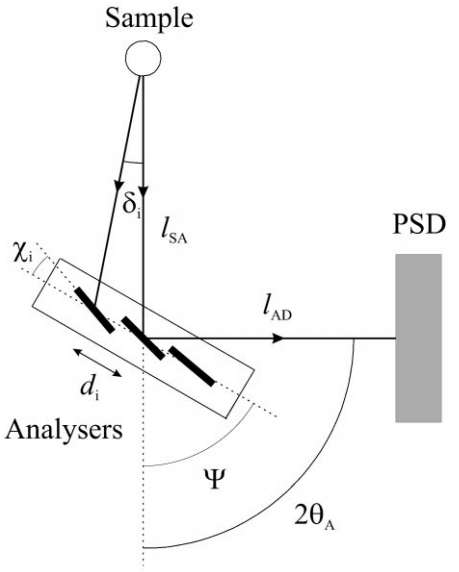

Fig. 1 . The essential parts of a flexible analyser assembly, including sample and detector, where the angles and distances of the secondary spectrometer are defined.

2.1. Focusing analyser modes

This group of modes contains the conventional TAS mode (A), i.e. a flat analyser, together with two modes, in the following named (B) and (C), where the beam is horizontally focused on to the detector. For all these modes, a single detector is sufficient to perform the experiment, although a PSD is useful to perform simultaneous measurements of data and the instrumental background, by masking out the relevant parts of the detector by software after the experiment. The analyser and detector configurations for these modes are shown in Fig. 2, along with a sketch of the resulting resolution function on RITA-1, as found by the Popovici option in RESCAL [8]. (For a more detailed investigation of the RITA resolution function, see Ref. [9].) For most modes, the RESCAL calculations were performed with no collimation. However, in modes where

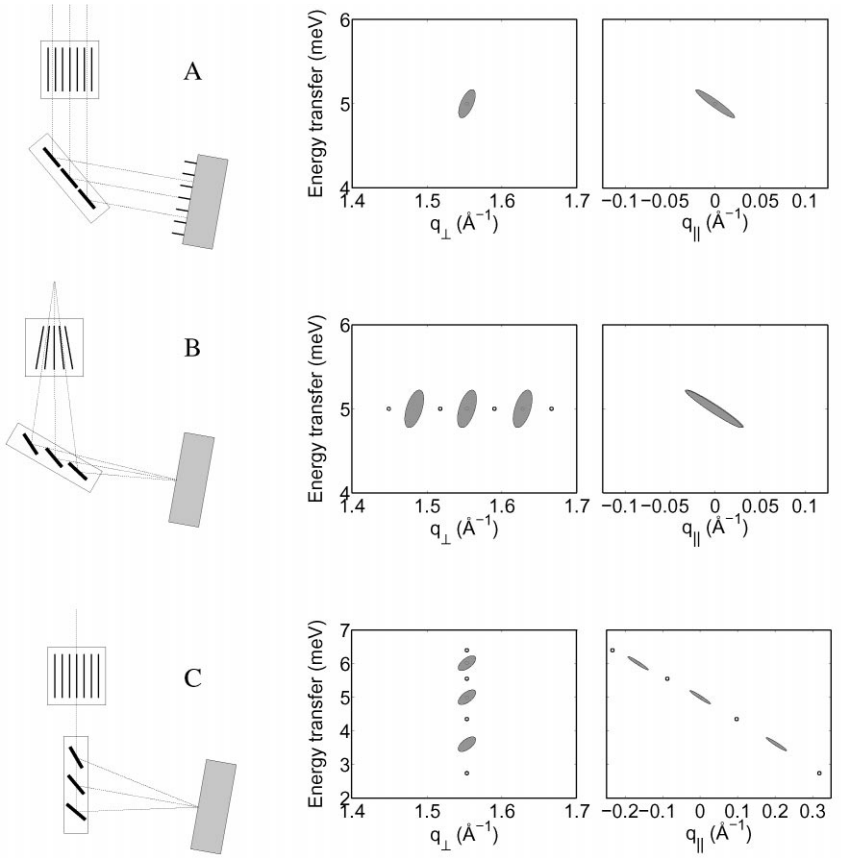

Fig. 2. A selection of focusing configurations of a multi-analyser secondary spectrometer. For all modes, the real-space configuration is shown (left) as well as projections of the resulting resolution function for RITA-1 (middle and right). For clarity, only three blades are shown on the real-space picture. For blades 2, 4, and 6, the full resolution ellipses are drawn, while for blades 1, 3, 5, and 7, only the centres of the resolution ellipses are shown. (A) The standard TAS mode, (B) Monochromatic point-to-point focusing mode, (C) Constant-$\boldsymbol{q}_\perp$ point-to-point focusing mode. For description of the modes, see text.

straight collimation is indicated, we have inserted a 60′ collimator. For the conventional TAS mode (A), we have used collimations of 60′ everywhere. The incoming neutron energy is 10 meV for all modes, and the central blade is set to $(\boldsymbol{q}, \hbar\omega) = (1.55\ \text{Å}^{-1}$ and 5 meV).

We choose a coordinate system for the scattering vector, $\boldsymbol{q} = \boldsymbol{q}_\perp + \boldsymbol{q}_\parallel$, where $\boldsymbol{q}_\parallel$ points along $\boldsymbol{k}_f$, the nominal wave vector of a neutron leaving the sample. Note that this definition differs from that of RESCAL, where $\boldsymbol{q}_\parallel$ points along the nominal scattering vector. In all the focused analyser modes, at least one of the two $\boldsymbol{q}$-components is constant. This reduces the essential part of the resolution function to two dimensions, which is not the case for all dispersive modes.

(A) is the conventional TAS mode with a flat analyser and straight collimators. In this mode, all analyser blades point along the assembly, $\chi_i = 0$, while the assembly itself is oriented as a usual single analyser: $\Psi = (2\theta_A)/2$. The flexibility of the analyser system may in this mode be used for optimizing the signal-to-noise ratio, by adjusting the effective width of the analyser [10].

(B) is the monochromatic point-to-point focusing mode, which corresponds to the horizontally

focusing analyser option, used at many TAS. The neutrons scattered over a large angular range impinge on the analyser blades. The "divergence angle", δ_i, is defined in Fig. 1, and is given by

$$\tan(\delta_i) = \frac{d_i \sin \Psi}{l_{SA} - d_i \cos \Psi} . \quad (1)$$

The blades are positioned to scatter neutrons, arriving from a point source, monochromatically and focus them onto a point (or rather: a vertical stripe) on the detector. This mode is frequently used both on SPINS [6], and on RITA-1 [11]. A radial collimator may be inserted before the analyser to reduce the background, but the resolution of this mode is given solely by distance collimation and by the analyser mosaicity. The rotation of the assembly is given by

$$\cot(\Psi) = \cot(2\theta_A) + l_{AD}/[l_{SA} \sin(2\theta_A)] \quad (2)$$

and the angles of the individual blades are found by

$$\Psi - \chi_i + \delta = \theta_A . \quad (3)$$

Eq. (3) ensures that the monochromatic condition is always fulfilled, while point focusing on the detector via Eq. (2) is only correct for $d_i \ll l_{SA}$ and $d_i \ll l_{AD}$. In this limit, the blades also scatter with constant $\boldsymbol{q}_\parallel$.

(C) is the constant-$\boldsymbol{q}_\perp$ point-to-point focusing mode. In mode (C), the analyser assembly points directly towards the sample, i.e. $\Psi = 0$, while the blades scatter neutrons of different energies onto the same point. The angles of the analyser blades are given exactly by

$$\tan(-2\chi_i) = \frac{l_{AD} \sin(2\theta_A)}{l_{AD} \cos(2\theta_A) - d_i} . \quad (4)$$

This mode has been used for one experiment on RITA-1 [12]. A straight collimator may be inserted before the analyser to reduce background – and to some extend improve the $\boldsymbol{q}_\perp$ resolution.

2.2. Dispersing analyser modes

In the dispersive modes, the imaging property of the PSD is used simultaneously to collect different data points, as each analyser blade directs neutrons onto a different part of the detector. Unused parts of the detector may be used to determine the background values. In general, a whole continuum of modes are possible, and we only present a few cases, either in current use or suggested elsewhere. In Fig. 3, we show selected positions of the blades, both in real space and in ($\boldsymbol{q}$, $\hbar\omega$) space.

(D1)–(D2) denotes two of the possible monochromatic dispersive modes, which all have (almost) constant-$\boldsymbol{q}_\parallel$. For both modes a radial colimator may be inserted after the sample to reduce the background. None of these modes have been tried on RITA-1.

(D1) is the monochromatic $\boldsymbol{q}_\perp$-dispersive mode in transmission geometry, as discussed in Ref. [1]. The analyser is arranged with $\Psi < 0$, and the neutrons are scattered at different blades at the same energy, but distributed over the PSD. In this mode, the points are more closely spaced in $\boldsymbol{q}_\perp$ than in (D2).

(D2) is the monochromatic $\boldsymbol{q}_\perp$-dispersive mode in reflection geometry, similar to mode (B). The analyser is set up to focus the beam horizontally *before* the PSD. A slit is inserted at the focusing point to reduce background. The angles of the analyser assembly and of the different blades in (D2) are as in Eqs. (2) and (3), where l_{AD} is replaced by the analyser-slit distance.

(E1)–(E3) denotes three special cases of a whole variety of non-monochromatic dispersive modes, of which much is still to be discovered.

(E1) is the energy-dispersive flat analyser mode. The analyser is positioned as in the standard TAS configuration (A), i.e. $\chi_i = 0$. However, no straight collimation is used, so neutrons scattered at different angles from the sample may contribute, if they have different energies. To utilize this, a radial collimator is placed before the PSD to make clear

Fig. 3. A selection of dispersing configurations of a multi-analyser secondary spectrometer, showing the real-space configurations (left) and the resolution functions (middel and right) (D1) Monochromatic $\boldsymbol{q}$-dispersive mode in transmission geometry, (D2) Monochromatic $\boldsymbol{q}$-dispersive mode in reflection geometry, (E1) Flat analyser energy-dispersive mode, (E2) Constant-$\boldsymbol{q}_\perp$ energy-dispersive mode, (E3) Energy-dispersive line focusing mode. For description of the modes, see text.

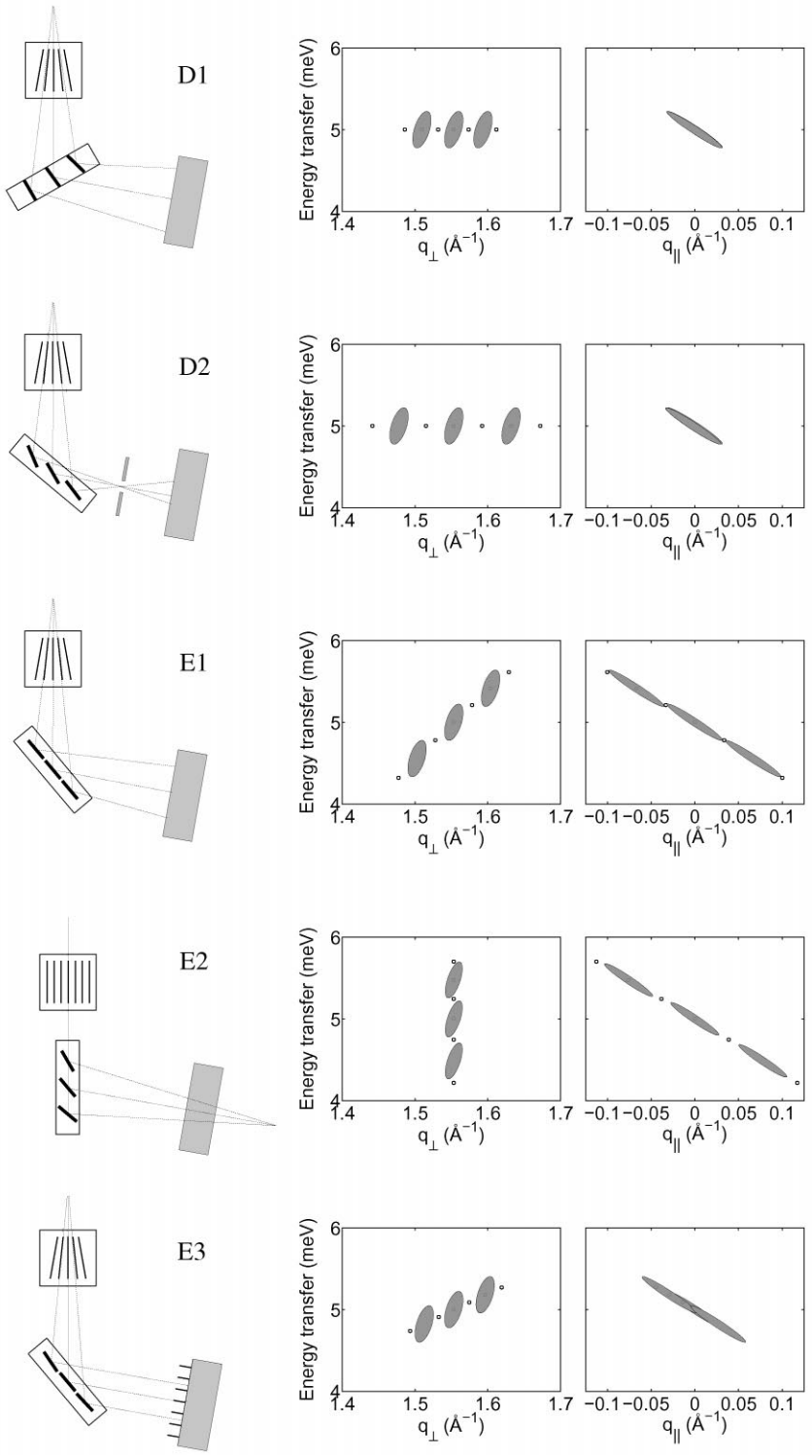
D1
D2
E1
E2
E3
Energy transfer (meV)
6
5
4
1.4
1.5
1.6
1.7
$q_\perp$ (Å^{-1})
−0.1
−0.05
0
0.05
0.1
$q_\parallel$ (Å^{-1})

assignments of different sections of the analyser to coresponding areas on the detector. This mode is the most used on the SPINS spectrometer [6], where it has been used to map out excitation continua, e.g. in the frustrated spin system of $ZnCr_2O_4$ [13]. A radial collimator may be used before the analyser to reduce background.

(E2) is the constant $\boldsymbol{q}_\perp$ energy-dispersive mode, similar to mode (C). The neutrons enter through a straight collimator, and the analyser assembly points towards the sample, $\Psi = 0$, while each blade scatters a different neutron energy. The resulting position of the blades is given by

$$\tan(-2\chi_i) = \frac{l_{\mathrm{AD}} \sin(2\theta_{\mathrm{A}}) - l_i \cos(2\theta_{\mathrm{A}})}{l_{\mathrm{AD}} \cos(2\theta_{\mathrm{A}}) + l_i \sin(2\theta_{\mathrm{A}}) - d_i}\,, \quad (5)$$

where l_i is the required position of the image of blade i on the PSD. In the limit $l_i = 0$, the focusing mode (C) is reached. A useful constraint in the present mode is to require the images of the blades on the detector to be equidistant. This was used in one RITA experiment on the ion conductor AgBr [14], see Section 3.5. The blade angles may also be found by Eq. (4), with l_{AD} replaced by a larger value to give a virtual focus point behind the PSD. This, however, does not in general provide equidistant images of the blades.

(E3) is the energy dispersive line focusing mode, as suggested in Ref. [7]. The neutron beam from the sample to the analyser assembly is allowed to diverge, while the beam from the analyser to the PSD passes a straight Soller collimator. This requirement leads to the following expression:

$$2(\Psi - \chi_i + \delta_i) = 2\theta_{\mathrm{A}} + \delta_i\,, \quad (6)$$

where δ_i is given by Eq. (1). The assembly angle Ψ may be varied freely to select the positions of the blades in $(\boldsymbol{q}, \hbar\omega)$ space, see one possibility in Fig. 3, in which Ψ has been chosen to 30°. This mode has never been tried on RITA-1.

When the system under investigation is low dimensional, the sample may always be oriented so that either $\boldsymbol{q}_\parallel$ or $\boldsymbol{q}_\perp$ is an irrelevant direction. In these cases, the constant-$\boldsymbol{q}_\perp$ modes (C) and (E2), or the constant-$\boldsymbol{q}_\parallel$ modes (B), (D1), and (D2) in effect can be made constant-$\boldsymbol{q}$ modes, easing the interpretation of the results. For the low-dimensional systems, modes (E1) and (E3) are mapping modes, which covers an arc which may be swept over the resulting $(q, \hbar\omega)$ plane.

The modes described above only cover a narrow selection of the possibilities. It is in fact possible to compromise between methods, in effect creating new options. One may, for example, interpolate between the methods (B) and (C), giving a focusing mode, which is matched to a particular dispersion relation. Also for the energy dispersive modes, much is still to be learned. There are even more ways of utilizing the flexibility of a multi-analyser system. One option is a TAS-like configuration with $\Psi = 0$, where all blades scatter at the same energy, $\chi_i = (2\theta_{\mathrm{A}})/2$ in order to improve the total reflectivity of the analyser. Another option is a non-elastic two-axis mode, which has been used in a recent RITA-1 experiment on CFTD [15], see Section 3.5.

3. The present RITA-1 spectrometer

The RITA-1 spectrometer has been designed for experiments which require high cold-neutron flux (in the range 3.6–25 meV) and a low background, while being able to tolerate a relaxed resolution. Schematic drawings of the spectrometer have been published earlier and much has been written about the primary spectrometer design [1–3]. Hence, the presentation of that part is restricted.

3.1. The primary spectrometer of RITA-1

From the cold source, the neutrons pass through a sapphire filter, an $m = 3.4$ supermirror guide section, and a motorized straight Soller collimator (20′, 40′, 60′, or open). A broad-bandpass velocity selector is then used to suppress higher order contamination of the incident beam. The 9-bladed 90′ PG monochromator may be focused vertically. A constant-focus 3-piece Heusler monochromator is planned to be mounted on the same turntable, displaced vertically, in order to ease a change to polarized neutrons during an experiment. After the monochromator, the neutrons travel through two guide sections, focusing onto the sample position. The mounts for the guide sections are magnetized

to provide guide fields for the polarized beam option. The second guide section may be replaced by a straight Soller collimator (15′, 30′, or 60′). The size of the beam at the sample position is 1.5×3 cm^2 with a collimator and 4×4 cm^2 with the second guide section.

Motorized B_3N_3 slits are positioned both before and after the sample. The sample itself is placed in the proper sample surroundings on a table, where rotation, translations, and tilts are all motorized. The maximum cryostat dimensions is approximately given by our Oxford 9 T magnet with a height of 150 cm, an outer diameter at the lower part of 44 cm, and a weight of 450 kg. To reduce background, e.g. from incoherent elastic scattering, a Be or BeO filter may be placed after the sample; if no filter is used, a larger cryostat diameter is possible. Within the filters we have options for straight or radial collimation, which both reduce multiple scattering, thus improving the discrimination factor and the small-angle background.

3.2. Performance of the RITA-1 primary spectrometer

During the first two years of operation, the flux on the sample position was found to decrease by a factor 2–3, depending on wavelength. Inspection of the inner supermirror guide sections revealed considerable radiation damage [3], but a replacement did not restore the initial flux. A pinhole imaging of the incoming beam, using a perfect-crystal Si monochromator, revealed that the beam was blocked close to the cold source, except for the very top and bottom parts. A subsequent replacement of the cold source plug insert did indeed restore the flux to its initial value; the present flux at the sample position, measured by Au foil activation, is 1.6×10^7n/(s cm^2) at 5 meV and 2.5×10^7 n/(s cm^2) at 12 meV. We believe that the blockage of the beam was caused by radiation damage to polyethylene, which caused it to swell and in turn made the inner lead flight tube collapse inwards.

3.3. The secondary spectrometer of RITA-1

The secondary spectrometer of RITA-1 is contained within a stainless-steel tank, which is covered on the outside by a 20 cm layer of a mixture of polyethylene and boric acid, and with 5 mm boron-containing plastic on the inside, to reduce background, especially from fast neutrons. This is important, since the RITA-1 detector is only 5–6 m from the reactor core. After improving the shielding in the bottom of the tank, the fast-neutron (beam-blocked) background in the whole 12×17 cm^2 PSD is now as low as 6 counts/min for a typical position. The tank opening is sealed by a sapphire window, as the tank has been constructed to run under vacuum to avoid air scattering due to the incoherent cross section of N_2, which scatters 5% of the beam per metre at ambient pressure. However, the first tests have shown problems with overheating of the detector electronics in vacuum, and our plan is now to run with a controlled He atmosphere. The tank entrance has a mount for 10.2 cm high collimators, of which a wide variety of both straight and radial is available. This collimator may be aligned by a motor.

The 7-blade horizontally focusing RITA analyser assembly is placed inside the tank, 99.0 cm from the centre of the sample table. Each blade consists of 4 PG (0 0 2) crystals with 30′ mosaicity. These pieces are mounted on a 2.5×15 cm^2 Al plate (blade 1 and 7 are slightly smaller in the vertical direction). The distance between the axes of adjacent blades is 2.6 cm. The PSD has an area of 12×17 cm^2 and may be placed either in landscape or in portrait mode, the latter being the most used option. The PSD is placed in a Cd beam channel, which also serves as a mount for a 15.2 cm tall straight or radial collimator. The analyser–detector distance is 28.2 cm.

3.4. Software for RITA-1

For running RITA-1, a number of software packages are available, which are under continuous development. Essential in this respect is the Risø spectrometer control program TASCOM [16], which is extendable using a macro-language and is very convenient for developing new configurations of the secondary spectrometer. Other packages, used both on RITA-1 and on our other spectrometers, include the online data aquisition (ODA) [17], which displays measurement results on a web

browser, and the data manipulation and fitting package Mview/Mfit [8]. The latter has been expanded with a (preliminary) facility for PSD picture analysis: psd_ctrl [18]. This program bins the counts obtained in a scan into a three-dimensional space spanned by the vertical and horizontal PSD pixel coordinates and the scan variable. The basic purpose of the program is to perform cuts in and integrations of this count-density; some of its functionality is shown in Section 3.5. For a more detailed analysis of experimental data, we are developing the Monte Carlo ray-tracing package McStas [19–21]. This program is capable of performing a complete, realistic simulation of RITA-1. The first simulated resolution functions of RITA-1, in mode (B), are shown in Ref. [20].

3.5. Examples of RITA-1 experiments

Due to various start-up problems and a few very time consuming experiments, the number of published RITA-1 experiments is somewhat limited. We here show two examples of data taken at RITA-1; for other examples see Ref. [3].

Fig. 4 shows measurements on a powder of the ion conductor AgBr [14]. The data were taken in

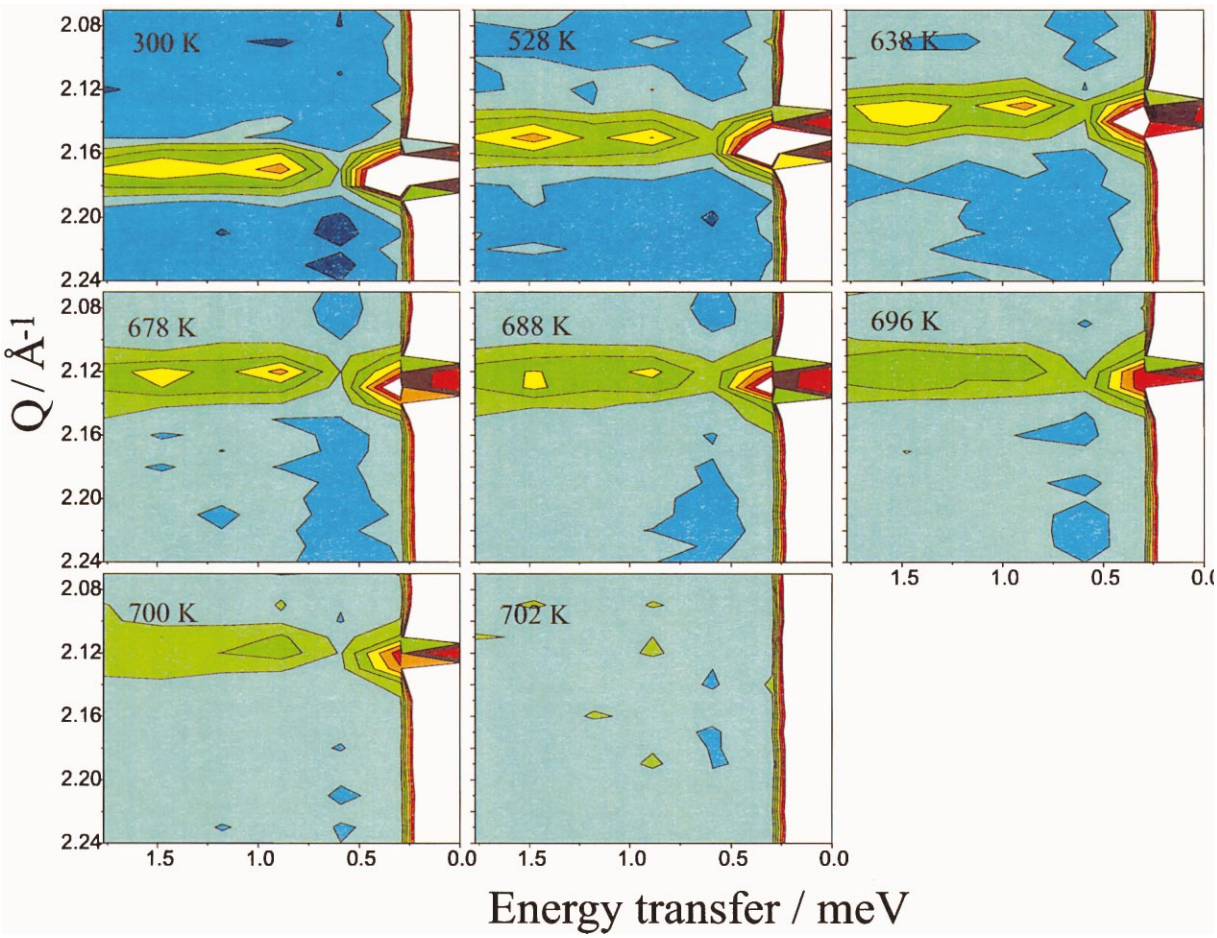

Fig. 4 . Typical inelastic data from RITA in the (E3) mode in an experiment on the ion conductor AgBr, where the melting point is 701°C. Blue and green colors represent low values, medium values are yellow through red, and high values are white, black and a few other colors (seen only close to zero energy transfer). In each measurement, six energy values were detected simultaneously, while one blade was unused. Each picture was obtained by a single q-scan; the q-value shown correspond to the nominal q for the elastically scattered neutrons. Figure adapted from [12].

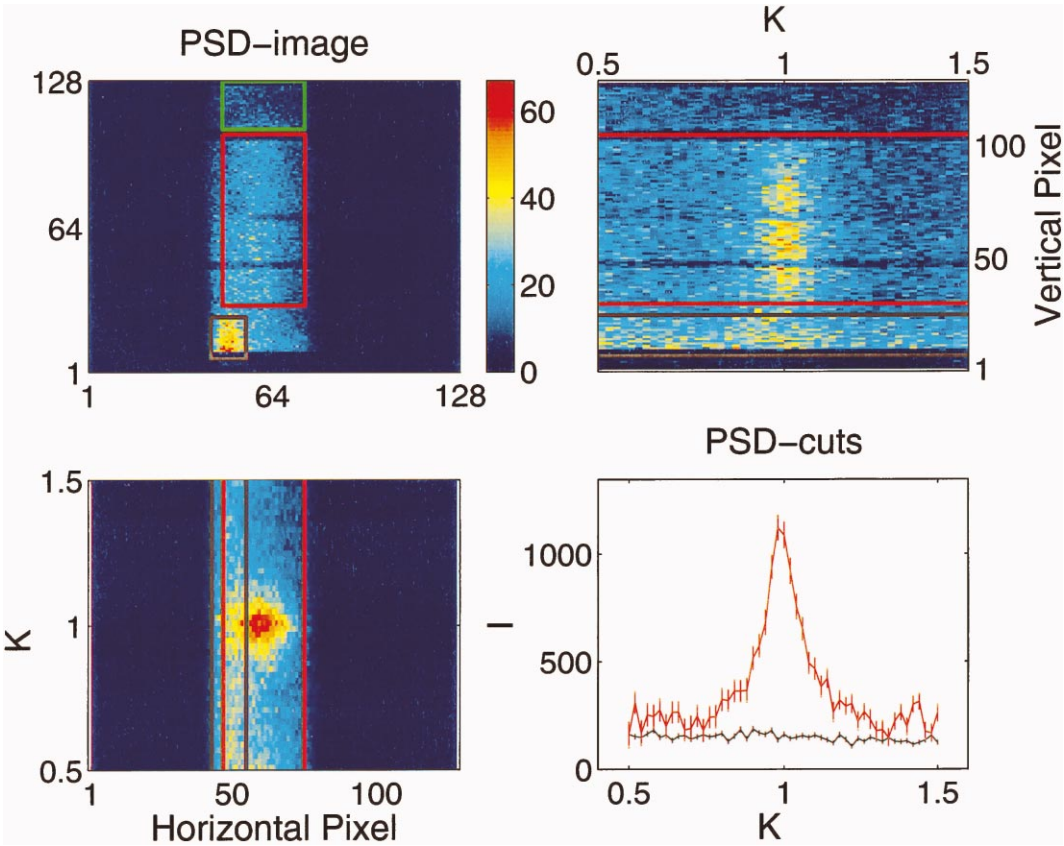

Fig. 5. The screen output from the program psd_ctrl, containing data for the $s = 1/2$ two-dimensional Heisenberg antiferromagnet CFTD [13]. Top left: Sum of all PSD counts within one scan. Top right: vertical sum of PSD pixels *vs.* the scan variable, k. Bottom left: horizontal sum of PSD pixels versus k. Bottom right: Sum of PSD counts (see text) versus k.

mode (E2), in which blade 7 was set to scatter elastically, and blade 6 was not in use, while blade 1–5 covered the inelastic response. The scattering angle, 2θ was scanned in order to cover an area of $(q, \hbar\omega)$ space, as shown in Fig. 4. The value of q given in the figure corresponds to blade 7 only. The measurements were performed at various temperatures close to the melting point of AgBr at 701°C. The positions and intensities of both the elastic and the inelastic signals were seen to vary with temperature, suggesting that the system approaches a second-order transition to a fast ion conducting phase at 705°C.

Fig. 5 shows inelastic data on the two-dimensional $s = \frac{1}{2}$ Heisenberg antiferromagnet CFTD, as displayed by the program psd_ctrl [15]. The spectrometer was in two-axis mode with a straight collimator; a constant-$\boldsymbol{q}_\perp$ mode. Ψ was set to a small angle, and all analyser blades were set to scatter away the background from elastic incoherent scattering. In this way, the beam was transmitted through several analyser blades before reaching the PSD. The sample was aligned so that its irrelevant direction (perpendicular to the antiferromagnetic planes) was being held in the $\boldsymbol{q}_\parallel$ direction. Hence, this configuration effectively gave an energy-integrated measurement with constant $\boldsymbol{q}$ – with a strongly suppressed contamination from the incoherent scattering. The scan in Fig. 5 is taken along $(k, k, 0)$, where $(1, 1, 0)$ is the antiferromagnetic point. The upper left panel shows the sum of all PSD counts in the whole scan, while

the top right and bottom left panels show the k-dependence of the vertical and horizontal coordinates of the counts, respectively. The PSD picture in the top left panel also contains markings for three rectangular windows, which are set interactively to a typical signal position (red), an expected background position (green), and a clear localized signal (black). The sum of counts within each of these windows were then normalized to the corresponding solid angle. In the lower right panel, we show the signal minus background (red) and the localized feature (black). The localized signal does not depend on k and is therefore most likely spurious. The counts in the expected signal window, on the other hand, does show the expected k dependence. These data enabled determination of the temperature dependence of the correlation length in the two-dimensional spin system [15].

Other experiments in the period from commisioning till late 1999 include the study of spin fluctuations in the high-T_C superconductor $La_{2-x}Sr_xCuO_4$ [21], observation of superparamagnetizm and collective magnetic excitations in α-Fe_2O_3 and γ-Fe_2O_3 nanoparticles [10,22], and magnetic excitations in the high-T_C superconductor $PrBa_2Cu_3O_{6+x}$ [23].

4. Design of the RITA-2 spectrometer

The RITA-2 spectrometer is meant for high-resolution experiments using a moderate flux of cold neutrons, of the order 1×10^7 n/(s cm^2), in the range 2.5–14 meV, combined with an extremely low background. RITA-2 is in many ways similar to RITA-1, and here we only list the essential differences.

RITA-2 will replace the existing TAS7 instrument in the Risø neutron guide hall, into which a curved guide leads neutrons from the cold source. No collimation before the monochromator is possible, whence the primary spectrometer resolution is limited by the monochromator mosaicity. There will be two monochromator options: vertically

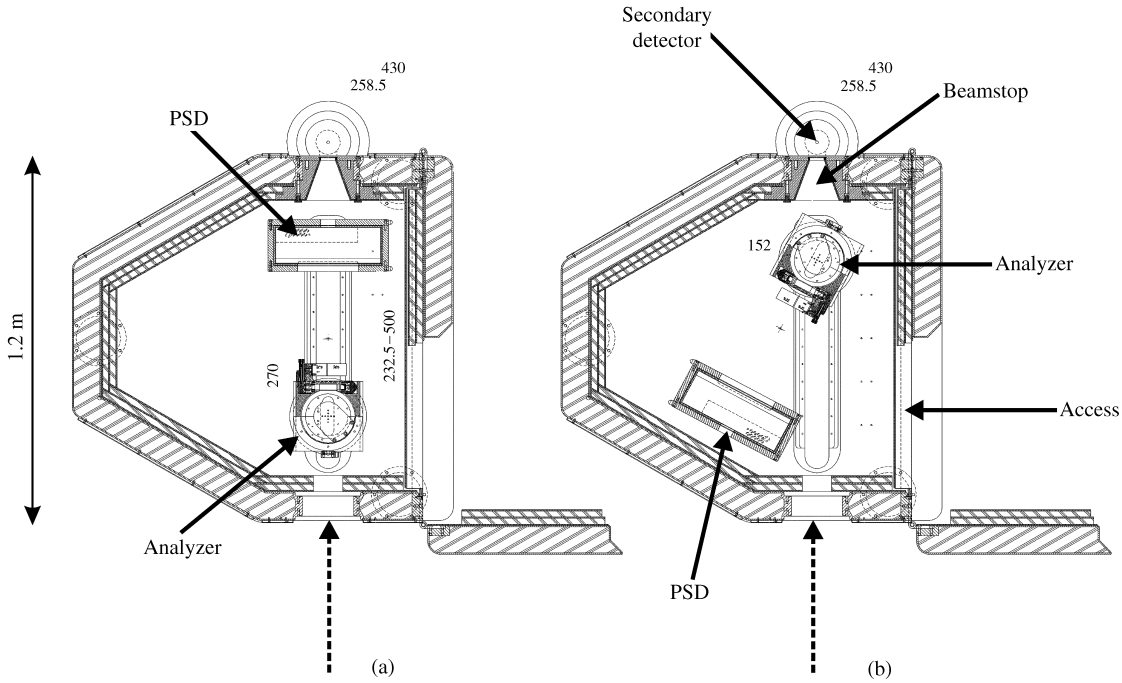

Fig. 6. Top views of RITA-2 with the side door open. (a) two-axis (and normal TAS) configuration, (b) backscattering TAS configuration. Possible analyser modes are not indicated.

focusing PG (0 0 2) with 30′ mosaicity, and Ge (1 1 1) with a horizontal mosaicity of 10′ and a vertical mosaicity of 20′. For the latter monochromator, second-order contamination is absent, as Ge (2 2 2) is a forbidden reflection.

The secondary spectrometer of RITA-2 is contained in an Al tank, and is intended to run in a He atmosphere at ambient pressure. The entrance to the tank is through a door in one side, providing easier access than the heavy lid on top of RITA-1. The tank shielding is similar to that of RITA-1, providing an extremely low fast-neutron background due to the long distance (25 m) to the reactor core. The analyser assembly is similar to RITA-1, but has 9 blades of either 30′ PG (002) or 15′ Ge (1 1 1) mounted on Si single crystals. The analyser assembly is able to move, allowing near-backscattering on the analyser side, as seen in Fig. 6. The reflection indices of the Ge analyser may be selected among several options to allow for backscattering at several energies. The main detector will be a 30×50 cm^2 PSD with a 7 mm (FWHM) spatial resolution. Further, a single detector will be placed in two-axis position in the beam stop of the tank.

5. Other flexible triple-axis spectrometers

As mentioned in the introduction, the only running spectrometer with a multi-blade analyser, besides RITA-1, is SPINS at NIST. Its primary spectrometer is very similar to that of RITA-2. It is located at the end of a long neutron guide, limiting the beam divergence and thus the maximum monochromatic flux at the sample position, which is roughly a factor of two lower than that of RITA-1 [6]. The secondary spectrometer of SPINS consists of a tank with a 9-blade analyser and a PSD, quite similar to RITA-1. SPINS has been operational since 1995 (the PSD was installed in 1998) and has already produced much useful data, mostly in the flat analyser energy-dispersive mode (E1) [6]. The beam-blocked background of SPINS is at present 20–30 counts/min in the whole 20×25 cm^2 PSD, slightly higher per area than that of RITA-1. SPINS has a much used option for polarized neutrons, which however, does not utilize the multi-bladed analyser [24]. A new cold source will be installed at NIST in the early 2000, and a cold-neutron flux gain of a factor of two is expected [6]. This will make SPINS comparable to RITA-1 in incident flux.

There are plans at NIST to build a high-flux TAS with 30 double-crystal analysers and a doubly focusing monochromator within the next three years. The estimated flux of this instrument is larger than 10^8 n/(s cm^2) [6]. Oak Ridge National Laboratory has plans to build a multi-analyser TAS, somewhat similar to RITA-2.

In Europe, ILL is considering the construction of a flexible TAS. An upgrade of IN3 with a PSD and an analyser array [7] would make the secondary spectrometer of this instrument resemble that of RITA-1. The two instruments would complement one another, since IN3 is on a thermal source. Also the scheduled instrumentation for the FRM-II in München contains an advanced thermal spectrometer, PUMA, which has an option for a RITA-like multi-analyser system [25].

6. Conclusion

The construction and operation of a powerful TAS with a flexible secondary spectrometer has been successful for both RITA-1 and SPINS, and more RITA-like TAS are planned/being built at continuous neutron sources. It is, however, clear that there is still much to be learned about the operation and optimization of their respective secondary spectrometers and that advanced software is crucial for planning and performing experiments as well as for data analysis.

At pulsed sources, improvements are seen with powerful spectrometers like MAPS and the proposed upgrade of HET at ISIS. Here, detectors covering a significant fraction of the full solid angle make it possible to access large regions of ($\boldsymbol{q}$, $\hbar\omega$) space. If, however, the key to understanding a specific problem is buried in the behaviour close to a specific ($\boldsymbol{q}, \hbar\omega$) point, the vast information obtained with time-of-flight methods may be unsuitable, and a flexible TAS might prove more useful. Indeed, several important features of e.g. the magnetic excitations in the high-T_C cuprates have only been revealed through complementary experiments

on time-of-flight instruments and individually optimized TAS [21,26]. In conclusion, it seems promising to continue development of advanced neutron spectrometers, both on continuous and pulsed sources.

Acknowledgements

First of all, we would like to thank the technical staff at Risø National Laboratory, who have been essential for the construction of the two RITA spectrometers. T.E. Mason has made large contributions to the design of RITA-1. We have had useful discussions with C. Broholm about SPINS. Thanks to P. Zetterström for lending us the AgBr data, and to P. Böni for producing the supermirror guides for RITA-1.

This project has been supported by the EC-RTD project *Cold Neutron Optimization*, FMGE-CT98-0098, where we have benefitted from collaboration with H. Graf, Hahn-Meitner Institut, Berlin, and U. Steigenberger, ISIS.

References

[1] T.E. Mason et al., Can. J. Phys. 73 (1995) 697.
[2] K.N. Clausen et al., Neutron News 7 (4) (1996) 21.
[3] K.N. Clausen et al., Physica B 241–243 (1998) 50.
[4] S.-H. Lee, C.F. Majkrzak, J. Neutron Res. 7 (1999) 131.
[5] C. Broholm, Nucl. Instr. and Meth. A 369 (1996) 169.
[6] C. Broholm (1999), personal communication.
[7] A. Hiess, in: The Millennium Programme, Proposals for ILL's 5-year Development Programme, ILL Report SC 99-1, 1999.
[8] A.D. Tennant, D.F. McMorrow, www.ill.fr/tas/Matlab/doc/matprgs.html.
[9] K. Nielsen, K. Lefmann, in these Proceedings (NOP '99), Physica B 283 (2000).
[10] K. Lefmann et al. (2000), to be published.
[11] S. Coad, A. Hiess, D.F. McMorrow, G.H. Lander, G. Aeppli (2000), to be published.
[12] Guangyong Xu (1999), personal communication.
[13] S.-H. Lee et al., cond-matt/9908433, 1999.
[14] P. Zetterström, A. Chahid, R.L. McGreevy, Physica B 266 (1999) 115.
[15] H.M. Rønnow, D.F. McMorrow, A. Harrison, Phys. Rev. Lett. 82 (1999) 3152.
[16] J. Bundgård, K.M. Enevoldsen, P. Skaarup, TASCOM Version 3.0, Reference Manual, Risø National Laboratory, Denmark, 1995.
[17] K. Nielsen, unpublished.
[18] H.M. Rønnow, unpublished.
[19] K. Lefmann, K. Nielsen, Neutron News 10 (3) (1999) 20.
[20] The McStas home page: http://neutron.risoe.dk/mcstas.
[21] B. Lake et al., Nature 400 (1999) 43.
[22] M.F. Hansen et al., Phys. Rev. Lett. 79 (1997) 4910.
[23] S.J.S. Lister et al., Physica C 317/318 (1999) 572.
[24] S.-H. Lee, C. Broholm (2000), to be published.
[25] The FRM-II home page www.frm2.tu-muenchen/d/instrumente/damf/rahmen.html.
[26] R. Coldea et al. (2000), to be published.